



11th International Symposium on Plasticity and Impact Mechanics, Implast 2016

## Effects of the addition of the inelastic fibers on the energy dissipation in the composite cantilever beam

Luv Verma<sup>a\*</sup>, Srinivasan M. Sivakumar<sup>a</sup>, S.Vedantam<sup>b</sup>

<sup>a</sup>Dept. of Applied Mechanics, Indian Institute of Technology (IIT), Chennai, Tamil Nadu, 600036, India

<sup>b</sup>Dept. of Engineering Design, Indian Institute of Technology (IIT), Chennai, Tamil Nadu, 600036 India

---

### Abstract

Present work deals with the analysis of the variation in the stresses of an inelastic composite cantilever beam. The cantilever beam is made up of four bi-directional symmetrically stacked glass-fiber/epoxy (GFRP) laminas. The stress field in the beam has been calculated using one dimensional finite element formulation of the Timoshenko beam theory. GFRP are the elastic composites and their behaviour is brittle. Thus the energy dissipation is generally given by the area under the elastic curve. The addition of the inelastic fibers in the composite extend this area after the yield stress leading to the more energy dissipation. To achieve an increase in the energy dissipation, aluminium (Al.) has been introduced as an inelastic fiber in the top-most layer and is considered to undergo kinematic hardening. Finite element formulation has been done for the aluminium reinforced glass fiber/epoxy composite cantilever beam. At small loads, even an incremental increase in the plastic area can be beneficial. The overall stiffness of the top-most layer is calculated by the rules of mixtures (Voigt) method and updated once stresses reach in the inelastic zone. As the top and the bottom most layer is made up of same composite material but the only difference is that of inelastic fibers in the top most layer, we can compare the stresses and how much energy dissipation increases in the top-most layer. The effect of varying the thickness on the stresses and energy dissipation is discussed.

© 2017 The Authors. Published by Elsevier Ltd. This is an open access article under the CC BY-NC-ND license (<http://creativecommons.org/licenses/by-nc-nd/4.0/>).

Peer-review under responsibility of the organizing committee of Implast 2016

*Keywords:* Energy dissipation, Cantilever beam, Inelastic composit

---

\* Corresponding author. *Email address:* [luvverma2011@gmail.com](mailto:luvverma2011@gmail.com)

## 1. Introduction

Composite materials are the future materials. They have replaced the conventional materials in many industries such as aerospace, automobiles and civil applications. With the time, the behavior of the composite is understood better and the capabilities of modelling them under various loading conditions increases. Though better than metals under longitudinal loading, composites are still finding the way to beat metals when they undergo impact loading. As they are brittle in nature, under impact they behave poorly. They generally fail in various modes [1], the extent of damage might even go unnoticed and thus the reliability reduces. For the impact applications such as car bumpers and a vehicle body, where more than damage to a vehicle, human life is at risk and dissipation of the energy through various modes is a primary important factor, composites generally cease to deliver.

To increase the energy dissipation of the components used in various applications as well as to reduce the weight at the same time, composites can be embedded with the materials with high dissipation capabilities. Drop weight impact testing has been done to provide the comparative results of the damage resistance in different types of the material [2]. Some work has been done on the energy dissipation using the metal matrix composites (MMCs) [3]. Low velocity impact on GFRP composites has been investigated by many researchers [4-6]. At low-velocity impact the dynamic response of the composite material has been analyzed and it has been observed that the matrix properties govern the damping behavior [7]. Finite element formulation using one dimensional (1-D) composite beam using Timoshenko beam theory has been given in many references [8-9]. The studies by different researchers have been conducted on how to dissipate energy under impact. Modelling of the energy dissipation as a function of the strain energies stored in the material directions of the composite materials has been done considering the first-order laminate theory including the transverse shear effects [10]. The damping properties of the thick composite laminates have been done by studying the changes in the constituent properties such as fiber volume ratio, fiber orientation, laminate configuration [11].

MMCs and ceramic composites are generally ductile because of matrix properties but loses the advantage of less weight. It is easy to calculate by homogenization procedure that adding materials such as viscoelastic in comparison to metals or alloys degrade the stiffness of the overall obtained materials as their modulus values are generally lower. Also, if the material is embedded in between, the impact load damages the front composite layers before coming in contact with the embedded energy dissipating material.

In this paper, attempt is made to develop a model for an approach to increase dissipated energy by embedding ductile fibers in the composite as longitudinal fibers. These fibers are embedded in the top-most layer of the composite material which directly faces the impact loads. To model this kind of behavior under impact, a cantilever composite beam with four bidirectional symmetric layers is considered to be embedded with the aluminum (Al.) as the fibers and the beam undergo loading at the end. After reaching yield stress, the Al. fiber will undergo plastic deformation and dissipates energy as can be seen from the area in the inelastic region of stress-strain curve. The composite model for 1-D inelastic beam using Timoshenko beam theory is derived. It is considered that the incremental force is applied transversely to the beam in steps. The finite element formulation is presented for the same. The laminas considered are oriented in 0/90/90/0 to avoid the axial-bending coupling. The paper has considered the Voigt process to calculate the overall property of the first lamina of composites and then calculate the overall stresses into all laminas.

The paper is organized as follows. In section two, we have discussed the inelastic finite element formulation and the algorithm to calculate the stress field in one dimension, in all the four laminas. In section three we have shown the effect of variation in thickness on the energy dissipation and stress-strain behavior.

## 2. Finite element formulation and Algorithm

The general form of the principle of virtual work (PVW) is given in the (Eq. 1). The right-hand side (R.H.S) represents the external force due to the point loads acting on the structure. The summation in the R.H.S corresponds to the nodal displacements and the transverse forces.

$$\int_V \delta \boldsymbol{\varepsilon}^T \boldsymbol{\sigma} dV = \sum_i \delta w_i P_{z_i} \quad (1)$$

In the finite element formulation, we consider that for one-dimensional beam there are two strains, that are longitudinal strain and shear strain. Considering one dimensional element, with each one having two nodes, each node has three degrees of freedom (D.O.F). According to the Timoshenko beam theory, first D.O.F is the axial displacement of the beam axis ( $u_0$ ), the second is the transverse displacement ( $w_0$ ) of the beam axis and third is the rotation angle ( $\theta$ ). These 3 D.O.Fs can be related to the strains by the (Eq. 2) Axial and shear stresses are related to the corresponding strains by the (Eq. 3).

$$\boldsymbol{\varepsilon} = \begin{pmatrix} \varepsilon_x \\ \gamma_{xz} \end{pmatrix} = \begin{pmatrix} 1 & -z & 0 \\ 0 & 0 & 1 \end{pmatrix} \begin{pmatrix} \frac{\partial u_0}{\partial x} & \frac{\partial \theta}{\partial x} & \frac{\partial w_0}{\partial x} - \theta \end{pmatrix}^T = \mathbf{S} \hat{\boldsymbol{\varepsilon}} \quad (2)$$

$$\boldsymbol{\sigma} = \begin{pmatrix} \sigma_x \\ \sigma_{xz} \end{pmatrix} = \begin{pmatrix} E & 0 \\ 0 & G \end{pmatrix} \begin{pmatrix} \varepsilon_x \\ \gamma_{xz} \end{pmatrix} = \mathbf{D} \boldsymbol{\varepsilon} = \mathbf{D} \mathbf{S} \hat{\boldsymbol{\varepsilon}} \quad (3)$$

(Eq. 4), is the equation for the resultant stress which relates the axial force, bending moment and the shear force in the beam section to the generalized strain vector. (Eq. 5) reduces the three dimensional formulation of the work done in the PVW to one dimension by introducing generalized strain from (Eq. 2) and resultant stress from (Eq 4).

$$\hat{\boldsymbol{\sigma}} = \iint_A \mathbf{S}^T \boldsymbol{\sigma} dA = \left( \iint_A \mathbf{S}^T \mathbf{D} \mathbf{S} dA \right) \hat{\boldsymbol{\varepsilon}} = \hat{\mathbf{D}} \hat{\boldsymbol{\varepsilon}} \quad (4)$$

$$W = \int_V \delta \boldsymbol{\varepsilon}^T \boldsymbol{\sigma} dV = \int_{l^e} (\delta \hat{\boldsymbol{\varepsilon}})^T \hat{\boldsymbol{\sigma}} dx = \int_{l^e} (\delta \hat{\boldsymbol{\varepsilon}})^T \hat{\mathbf{D}} \hat{\boldsymbol{\varepsilon}} dx \quad (5)$$

The generalized constitutive matrix is given by  $\hat{\mathbf{D}}$ . In the matrix  $\hat{D}_a$ ,  $\hat{D}_b$ ,  $\hat{D}_{ab}$  represents axial stiffness, bending stiffness and axial-bending coupled stiffness.  $\mathbf{B}$  is the strain interpolation vector.  $B_{a_i}$ ,  $B_{b_i}$ ,  $B_{s_i}$  represents the axial, bending and shear strain interpolation terms.

$$\hat{\mathbf{D}} = \begin{pmatrix} \hat{D}_a & \hat{D}_{ab} & 0 \\ \hat{D}_{ab} & \hat{D}_b & 0 \\ 0 & 0 & \hat{D}_s \end{pmatrix}; \hat{\boldsymbol{\varepsilon}} = \mathbf{B} \mathbf{a}^{(e)}; \mathbf{B} = \begin{pmatrix} B_{a_i} \\ B_{b_i} \\ B_{s_i} \end{pmatrix} \quad (6)$$

Putting (Eq. 5, 6) in (Eq. 1), we get the PVW in one-dimensional form as follows:

$$\int_{I^e} (\delta \hat{\epsilon})^T \hat{D} \hat{\epsilon} dx = \int_{I^e} (B \delta a)^T \hat{D} (B a) dx = \delta a^T \left[ \int_{I^e} B^T \hat{D} B dx \right] a \tag{7}$$

The total number of laminas are denoted by  $n_l$ . The laminate axial, bending and shear stiffness are denoted by  $\hat{D}_a, \hat{D}_b$  and  $\hat{D}_{ab}$ . These stiffnesses can be calculated by first integrating them over the individual laminas area ( $A_k$ ) and then summing up the young's modulus and shear modulus over all the individual laminas in one-dimensional settings. Young's modulus is denoted by  $E_k(x, z_k)$  where  $k$  is a lamina index. Shear modulus of the  $k^{\text{th}}$  lamina is denoted by  $G_k(x, z_k)$ . Both of them are constant in a lamina but varies from one lamina to other.  $k_z$  represents the shear correction parameter. For (0/90) layout  $\hat{D}_{ab}$  is equal to zero.  $z_k$  represents the distance along of the  $k^{\text{th}}$  lamina along the  $z$ -axis from the reference considered in the middle of the four layers.

$$\hat{D}_a = \sum_{k=1}^{n_l} \int_{A_k} E_k(x, z_k) dA_k ; \hat{D}_b = \sum_{k=1}^{n_l} \int_{A_k} E_k(x, z_k) z_k^2 dA_k ; \hat{D}_s = \sum_{k=1}^{n_l} k_z \int_{A_k} G_k(x, z_k) dA_k \tag{8}$$

From (Eq. 7) and (Eq. 8), the expression below can be expanded and can be written for the individual composite laminas.

$$\delta a^T \left[ \int_{I^e} B^T \hat{D} B dx \right] a = \delta a^T \sum_{k=1}^{n_l} \int_{I^e} \left[ \{ B_{a_i}^T \left( \int_{A_k} E_k(x, z_k) dA_k \right) B_{a_i} \} dx \right] a + \dots \tag{9}$$

$$+ \left[ \{ B_{b_i}^T \left( \int_{A_k} E_k(x, z_k) z_k^2 dA_k \right) B_{b_i} + B_{s_i}^T \left( k_z \int_{A_k} G_k(x, z_k) dA_k \right) B_{s_i} \} dx \right] a$$

The significance of (Eq. 9), is that as in 0/90/90/0 layout only one of the four laminas is inelastic or having material non-linearity. Thus, we need to calculate the directional derivative of PVW for the top most lamina. Thus (Eq. 10), divides the above equation in three parts. The first term represents the linear part of the PVW for the first lamina. Thus, in the first term of the equation  $k$  is equal to one and thus subscript  $k$  is changed accordingly. The last term represents the PVW for all the other three laminas which are linear. The second term calculates the directional derivative of the first lamina of the composite and thus  $k$  is equal to one. The linear young modulus is replaced with the tangent modulus which is calculated at every time step and it represents incremental slope in one-dimensional.

$$\delta a^T \int_{I^e} \left[ \{ B_{a_i}^T \left( \int_{A_1} E_1(x, z_1) dA_1 \right) B_{a_i} + B_{b_i}^T \left( \int_{A_1} E_1(x, z_1) z_1^2 dA_1 \right) B_{b_i} \} dx \right] a + \dots$$

$$+ \delta a^T \int_{I^e} \left[ \{ B_{s_i}^T \left( k_z \int_{A_1} G_1(x, z_1) dA_1 \right) B_{s_i} \} dx \right] a + \left[ \{ B_{a_i}^T \left( \int_{A_1} E_1'(x, z_1) dA_1 \right) B_{a_i} \} dx \right] \Delta a +$$

$$W + D_{\Delta t} W = \dots + \delta a^T \int_{I^e} \left[ \{ B_{b_i}^T \left( \int_{A_1} E_1'(x, z_1) z_1^2 dA_1 \right) B_{b_i} + B_{s_i}^T \left( k_z \int_{A_1} G_1'(x, z_1) dA_1 \right) B_{s_i} \} dx \right] \Delta a + \dots \tag{10}$$

$$+ \delta a^T \left[ \sum_{k=2}^{n_l} \int_{I^e} \left[ \{ B_{a_i}^T \left( \int_{A_k} E_k(x, z_k) dA_k \right) B_{a_i} + B_{b_i}^T \left( \int_{A_k} E_k(x, z_k) z_k^2 dA_k \right) B_{b_i} \} dx \right] a + \dots \right]$$

$$+ \left[ \{ B_{s_i}^T \left( k_z \int_{A_k} G_k(x, z_k) dA_k \right) B_{s_i} \} dx \right] a$$

Taking the PVW for the composite earlier on the L.H.S to the R.H.S gives the unbalanced force vector.  $r_l$  is an updated force with the new stress value in all the laminas and thus the subtraction of the  $r_l$  from the external force on the node denoted by  $P_n$  gives the unbalanced force. The convergence criteria can be set. (Eq. 10), gives incremental displacement ( $\Delta a$ ), using which we can calculate the increments in the three nodal degrees of freedoms.

$$D_{\Delta t} W \Delta a = -r_l + P_n \tag{11}$$

Where

$$D_{\Delta t} W = \int_{A_1} [\{B_{a_i}^T (\int_{A_1} E_1'(x, z_1) dA_k) B_{a_i}\} dx] + \dots \tag{12}$$

$$+ \int_{A_1} [\{B_{b_i}^T (\int_{A_1} E_1'(x, z_1) z_1^2 dA_1) B_{b_i} + B_{s_i}^T (k_z \int_{A_1} G_1'(x, z_1) dA_1) B_{s_i}\} dx]$$

$$r_l = \int_{r^e} (\delta \hat{\varepsilon})^T \hat{D} \hat{\varepsilon} dx = \sum_{k=1}^{n_l} \int_{A_k} [\{B_{a_i}^T (\int_{A_k} E_k(x, z_k) dA_k) B_{a_i}\} dx] + \dots \tag{13}$$

$$+ \int_{A_k} [\{B_{b_i}^T (\int_{A_k} E_k(x, z_k) z_k^2 dA_k) B_{b_i} + B_{s_i}^T (k_z \int_{A_k} G_k(x, z_k) dA_k) B_{s_i}\} dx]$$

The axial bending and shear tangent modulus stiffness tensors are denoted by  $K_{ai}'$ ,  $K_{bi}'$ ,  $K_{si}'$ . The total tangent stiffness tensor is a summation of the above three denoted by  $K'$ . The incremental displacements at the nodes can be found out by from (Eq. 14 or 15). F represents the total unbalanced force at every step.

$$(K_{ai}' + K_{bi}' + K_{si}') \Delta a = r_l + P_n \tag{14}$$

$$K' \Delta a = F \tag{15}$$

There are many homogenization techniques which can be employed to calculate the overall modulus of the first lamina as it consists of aluminum fibers embedded in glass-fibers epoxy. The simplest one is the Voigt method or the rules of mixtures which is the average of the tangent modulus of the matrix and the fibers weighted according to their volume fractions. The equation is given as follows:

$$E' = V_m \left(\frac{d\sigma}{d\varepsilon}\right)_m + V_f \left(\frac{d\sigma}{d\varepsilon}\right)_f = V_m E_m + V_f \left(\frac{d\sigma}{d\varepsilon}\right)_f \tag{16}$$

In the above equation, glass-fiber/epoxy is considered as a matrix (m), and aluminum as the fibers (f). The behavior of glass-fiber/epoxy is considered to be linear and thus model is governed by  $E_m$  which represents the Young's modulus of glass-fiber/epoxy of the first lamina. As aluminum fiber reaches the yield stress, incremental modulus needs to be considered which defines the ratio of incremental strain by incremental strain in the above equation. In the above equation, tangent modulus of the fiber is given as [13]:

$$\left(\frac{d\sigma}{d\varepsilon}\right)_f = \frac{E_{al} K_{al}}{E_{al} + K_{al}} \tag{17}$$

$E_{al}, K_{al}$  represents Young's modulus and the kinematic hardening modulus of the aluminium.

The above formulation gives the displacement at the nodes of an element and takes care of the global and local forces. To calculate the stresses in the 1<sup>st</sup> lamina which undergoes kinematic hardening and thus behave inelastically, the convex cutting plane algorithm [12] have been employed which takes the strain as an input at each load increment and gives out the stresses in the first lamina. The algorithm below completely describes the global picture from applying force increment to the calculation of stresses at the local and global level. The algorithm is given as follows:

1. Increment the load :  $F_{n+1} = F_n + F$
2. Find out the matrix A, B and D for the composite by calculating them for the individual laminas and summing them together using elastic, shear modulus and theta properties.
3. Find out the displacement, bending and shear stiffness  $K_a, K_b, K_s$
4. Solve  $K u = F$
5. Using the increments in displacement at every load step, calculate the total displacement at  $t_{n+1}$  by  $u_{n+1} = u_n + u$ .
6. Divide each lamina into three parts, and label them using z- indices starting from the top. So there are total 12 z-indices for four layered composite because at the boundary we need to define two indices.
7. At each z- position find out the strains  $\epsilon_{xx}, \gamma_{xz}$
8. The aluminum (Al.) fiber is embedded in the top-most layer, thus at  $z_1$  index material property is inelastic and hence strain at  $z_1$  is supplied to the 1-D kinematic convex cutting algorithm [12] function.
9. The Al. fiber is considered to undergo kinematic hardening when the yield function in the fiber becomes equal to or greater than zero. The function is supplied with strain and hence the algorithm is strain controlled locally and force-controlled globally.
10. After reaching critical yield stress, plastic strain, back stress and total stress is calculated in 1-D at every iteration. Based on critical yield stress value, the tangent modulus (Eq. 17) is calculated for the fibers.
11. After calculating tangent modulus, the Voigt method is used and based on the (Eq. 16), the overall tangent modulus of the composite is calculated and used to calculate A, B, D matrix for the first lamina in the following iteration consisting fibers.
12. The stresses can be calculated in the other laminas and corresponding indices using simple composite linear elastic relations.

### 3. Results

In the following section, results using finite element formulation has been shown for the composite with four laminas stacked as 0/90/90/0. The beam is considered to be a cantilever beam with the length divided into elements and each element is having two nodes. Each node has three degrees of freedom. Material properties and geometric properties of the element and the composite is given in Table 1. The width and thickness given in the dimension section belong to the cross-section of the composite.

Table 1. Material properties and dimensions of the beam.

Properties and Dimension	
Glass-fiber/epoxy	$E_1 = 38.6 \text{ GPa}, E_2 = 8.27 \text{ GPa}, \mu = 0.26,$ $G_{12} = 4.14 \text{ GPa}, G_{23} = 1.65 \text{ GPa}$
Aluminum (Al.) fiber	$E_{al} = 70 \text{ GPa}, \mu_{al} = 0.32$
Comp. Dimensions	$L_{elem} = 6.3 \text{ mm}, b = 40 \text{ mm}, t = 10 \text{ mm}$

Figures below show the stress variation along the thickness of the composite beam for three different thicknesses. The origin of the z-axis is considered to be a center of the composite. Fig. 1 shows the variation of the stress in the beam along its thickness. The stresses are symmetrical for the second and third laminas stacked at 90 degrees for all three cases of thickness. The stresses are not symmetrical in the first and fourth layer even they are at same angles. The reason is the addition of inelastic fibers in the top-most layer. In the modelling, homogenization of aluminum

fibers with GFRP increases the modulus property of the top-most lamina. Thus for the same amount of strain, the stresses are more in the top-most layer. It means that any embedment will increase the stresses in the composite in that specific region. Increasing the overall thickness increase the stresses in the laminas and is better explained by Fig 2. It shows one-dimensional stress vs strain plot in the longitudinal direction for different laminas oriented at different angles and for the overall thickness variation. After reaching yield-stress, the top most layer shows inelastic behavior due to the presence of inelastic fibers which undergoes kinematic hardening. The curve gives the overall behavior of composite. In the top-most layer, loading and unloading paths are different as evident by the hysteresis, thus giving the extra area in the plastic region that is not possible to get in the elastic composites and this lead to an increase in the energy dissipation. While unloading elastic composites retain their original states, and hence if unloading is a part of the phenomenon we are looking at, energy dissipation will be zero. Generally, in the impact events, the area under the loading curve is one which gives the dissipation to failure. As metal is embedded stresses are more in the embedded region giving an advantage even in an elastic region over non-embedded composites. The effect of thickness is evident from the increment in the energy dissipation. As thickness is less, the contact time of the sample with projectile will be less. As a result, the full potential of embedment won't come into play in terms of plastic dissipation. As thickness increases, the embedment will be in the contact time with the projectile will increase and hence plastic dissipation should increase with the thickness. Also, there is an elastic component of dissipation which is integrated in an implicit way with the metal fiber and hence total energy dissipation is more.

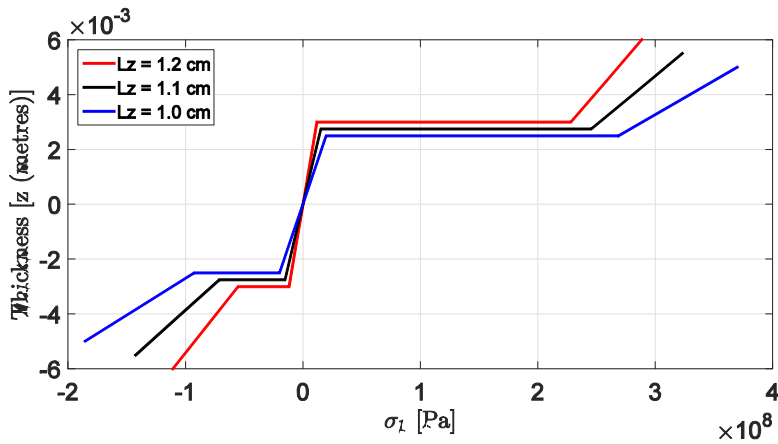


Fig. 1. Stress variation along the thickness direction for a particular load for 0/90s composite

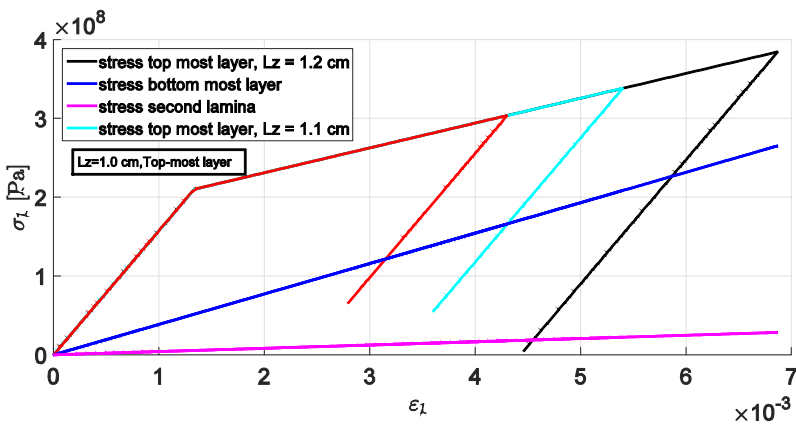


Fig. 2. Stress- strain variation along the longitudinal direction for different laminas with varying thickness

It is evident from Table 2, below that there is an overall increment in the top-most lamina energy dissipation on varying the overall thickness of the composite laminate as shown in Fig 2. and explained above. For elastic laminas with 0 and 90 degree orientation, variation in the energy dissipation is not considerable and thus they don't play major role in dissipation as compared to the first lamina

Table 2. Energy dissipation for various thickness and laminas

Thickness(cm)	Lamina no. or angle.	Energy dissipation (Pa)
1	Top most (1)	1.67e6
1.1	Top most (1)	2.36e6
1.2	Top most (1)	3.4e6
1	0 Deg. (4)	9.0e5
1	90 Deg. (2)	9.7e4

#### 4. Conclusion

In this paper, we have given a finite element formulation (FEA) for embedding inelastic fibers in the composites. An algorithm explains a procedure to solve a global force-controlled but locally strain-controlled problem for the inelastic composite laminate. Variation of the stresses due to the addition of metal fibers in the top-most lamina of the composite is discussed. It is shown that the stresses will be higher in the lamina with the fibers instead of the lamina with same orientation but without fibers. The variation of the thickness of composite laminate on the energy dissipation and the stresses has been discussed. It is also shown that embedding inelastic fibers and increasing thickness increases the amount of energy dissipation of the laminate.

#### References

- [1] Richardson, M. O. W., and M. J. Wisheart. "Review of low-velocity impact properties of composite materials." *Composites Part A: Applied Science and Manufacturing* 27.12 (1996): 1123-1131.
- [2] Naik, N. K., et al. "Impact and compression after impact characteristics of plain weave fabric composites: effect of plate thickness." *Advanced Composite Materials* 12.4 (2004): 261-280.
- [3] Jincheng, Wang, and Yang Gencang. "The energy dissipation of particle-reinforced metal-matrix composite with ductile interphase." *Materials Science and Engineering: A* 303.1 (2001): 77-81.
- [4] Ross, C. A., and R. L. Sierakowski. "Studies on the impact resistance of composite plates." *Composites* 4.4 (1973): 157-161.
- [5] Cantwell, W. J., and J. Morton. "The impact resistance of composite materials—a review." *composites* 22.5 (1991): 347-362.
- [6] Belingardi, Giovanni, and Roberto Vadori. "Low velocity impact tests of laminate glass-fiber-epoxy matrix composite material plates." *International Journal of Impact Engineering* 27.2 (2002): 213-229.
- [7] Zaretsky, E., and M. Perl. "The response of a glass fibers reinforced epoxy composite to an impact loading." *International journal of solids and structures* 41.2 (2004): 569-584.
- [8] Oñate, Eugenio. *Structural analysis with the finite element method. Linear statics: volume 2: beams, plates and shells.* Springer Science & Business Media, 2013.
- [9] Bhatti, M. Asghar. *Advanced topics in finite element analysis of structures: with Mathematica and MATLAB computations.* John Wiley & Sons, Inc., 2006.
- [10] Berthelot, Jean-Marie, et al. "Damping analysis of composite materials and structures." *Composite Structures* 85.3 (2008): 189-204.
- [11] Saravanos, D. A. "Integrated damping mechanics for thick composite laminates and plates." *Journal of Applied Mechanics* 61.2 (1994): 375-383.
- [12] Nallathambi, Ashok K., et al. "A 3-species model for shape memory alloys." *The International Journal of Structural Changes in Solids* 1.1 (2009): 149-170.
- [13] Simo, Juan C., and Thomas JR Hughes. *Computational inelasticity.* Vol. 7. Springer Science & Business Media, 2006.